Article

Positioning Lipid Membrane Domains in Giant Vesicles by Micro-organization of Aqueous Cytoplasm Mimic

Ann-Sofie Cans, Meghan Andes-Koback, and Christine D. Keating

J. Am. Chem. Soc., **2008**, 130 (23), 7400-7406 • DOI: 10.1021/ja710746d • Publication Date (Web): 15 May 2008

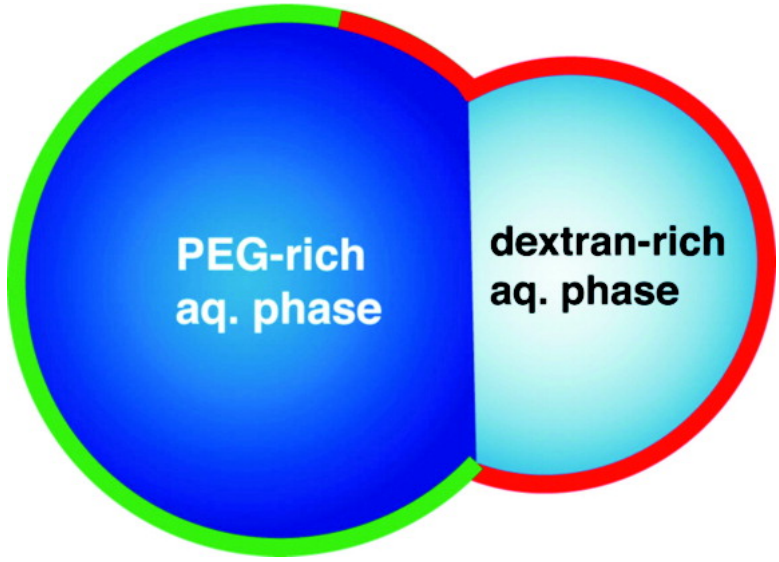

J|A|C|S
ARTICLES

Published on Web 05/15/2008

Positioning Lipid Membrane Domains in Giant Vesicles by Micro-organization of Aqueous Cytoplasm Mimic

Ann-Sofie Cans, Meghan Andes-Koback, and Christine D. Keating*

Department of Chemistry, The Pennsylvania State University, University Park, Pennsylvania 16802

Received November 30, 2007; Revised Manuscript Received March 25, 2008; E-mail: keating@chem.psu.edu

Abstract: We report localization of lipid membrane microdomains to specific "poles" of asymmetric giant vesicles (GVs) in response to local internal composition. Interior aqueous microdomains were generated in a simple model cytoplasm composed of a poly(ethyleneglycol) (PEG)/dextran aqueous two-phase system (ATPS) encapsulated in the vesicles. The GV membrane composition used here was a modification of a DOPC/DPPC/cholesterol mixture known to form micrometer-scale liquid ordered and liquid disordered domains; we added lipids with PEG 2000 Da-modified headgroups. Osmotically induced budding of the ATPS-containing GVs led to structures where the PEG-rich and dextran-rich interior aqueous phases were in contact with different regions of the vesicle membrane. Liquid ordered (L_o) membrane domains rich in PEG-terminated lipids preferentially coated the PEG-rich aqueous phase vesicle "body", while coexisting liquid disordered (L_d) membrane domains coated the dextran-rich aqueous phase "bud". Membrane domain positioning resulted from interactions between lipid headgroups and the interior aqueous polymer solutions, e.g., PEGylated headgroups with PEG and dextran polymers. Heating resulted first in patchy membranes where L_o and L_d domains no longer showed any preference for coating the PEG-rich vs dextran-rich interior aqueous volumes, and eventually complete lipid mixing. Upon cooling lipid domains again coated their preferred interior aqueous microvolume. This work shows that nonspecific interactions between interior aqueous contents and the membrane that encapsulates them can drive local chemical heterogeneity, and offers a primitive experimental model for membrane and cytoplasmic polarity in biological cells.

Introduction

Biological cells exhibit chemical heterogeneity in both their plasma membranes and their interiors.[1–5] In addition to obvious forms of heterogeneity such as the presence of membrane-encapsulated organelles and cytoskeletal structures in eukaryotic cells, the biochemical composition of the cytoplasm itself is nonuniform.[3,6] Although both cytoplasmic and membrane microcompartmentation are thought to be critical aspects of cellular structure, their origins and consequences are not yet well understood. Giant lipid vesicle (GV)[7–9] membrane model systems have incorporated lateral heterogeneity in the form of coexisting microscale lipid domains.[10] Relatively few cell models have yet been constructed that incorporate heterogeneous aqueous interiors; examples include GV containing hydrogels or small vesicles.[11–16] We recently reported a cytoplasm mimic based on vesicle-encapsulated aqueous solutions of poly(ethyleneglycol) (PEG) and dextran, which can separate into two coexisting aqueous phases.[15–17] Aqueous two-phase systems (ATPS) can form when two polymers or a polymer and a salt are mixed in water at sufficiently high polymer concentrations.[18–20] For example, in this work we encapsulate ATPS composed of

(1) Harold, F. M. *Microbiol. Molec. Biol. Rev.* **2005**, *69*, 544–564.
(2) Alberts, B.; Johnson, A.; Lewis, J.; Raff, M.; Roberts, K.; Walter, P. *Molecular Biology of the Cell*, 4th ed.; Garland Science: New York, 2002.
(3) (a) Parker, R.; Sheth, U. *Science* **2003**, *300*, 805–808. (b) Liu, J.; Valencia-Sanchez, M. A.; Hannon, G. J.; Parker, R. *Nat. Cell Biol.* **2005**, *7*, 719–723.
(4) (a) Jacobson, K.; Mouritsen, O. G.; Anderson, R. G. W. *Nat. Cell Biol.* **2007**, *9*, 7–14. (b) Del Pozo, M. A.; Schwartz, M. A. *Trends Cell Biol.* **2007**, *17*, 246–250. (c) Hancock, J. F. *Nat. Rev. Mol. Cell Biol.* **2006**, *7*, 456–462.
(5) (a) Baumgart, T.; Hammond, A. T.; Sengupta, P.; Hess, S. T.; Holowka, D. A.; Baird, B. A. *Proc. Natl. Acad. Sci. U.S.A.* **2007**, *104*, 3165–3170. (b) Davey, A. M.; Walvick, R. P.; Liu, Y.; Heikal, A. A.; Sheets, E. D. *Biophys. J.* **2007**, *92*, 343–355.
(6) Walter, H.; Brooks, D. E. *FEBS Lett.* **1995**, *361*, 135–139.
(7) Menger, F. M.; Angelova, M. I. *Acc. Chem. Res.* **1998**, *31*, 789–797.
(8) *Giant Vesicles*, Perspectives in Supramolecular Chemistry 6; Luisi, P. L., Walde, P., Eds.; John Wiley and Sons: West Sussex, 2000.
(9) Dimova, R.; Aranda, S.; Bezlyepkina, N.; Nikolov, V.; Riske, K. A.; Lipowsky, R. *J. Phys.: Condens. Matter* **2006**, *18*, S1151–S1171.
(10) Veatch, S. L.; Keller, S. L. *Biochim. Biophys. Acta* **2005**, *1746*, 172–185.
(11) Jesorka, A.; Markstrom, M.; Orwar, O. *Langmuir* **2005**, *21*, 1230–1237. (b) Markstrom, M.; Gunnarsson, A.; Orwar, O.; Jesorka, A. *Soft Matter* **2007**, *3*, 587–595.
(12) Viallat, A.; Dalous, J.; Abkarian, M. *Biophys. J.* **2004**, *86*, 2179–2187.
(13) Kiser, P. F.; Wilson, G.; Needham, D. *Nature* **1998**, *394*, 459–462.
(14) Bolinger, P.-Y.; Samou, D.; Vogel, H. *J. Am. Chem. Soc.* **2004**, *126*, 8594–8595.
(15) Long, M. S.; Jones, C. D.; Helfrich, M. R.; Mangeney-Slavin, L. K.; Keating, C. D. *Proc. Natl. Acad. Sci. U.S.A.* **2005**, *102*, 5920–5925.
(16) Long, M. S.; Cans, A.-S.; Keating, C. D. *J. Am. Chem. Soc.* **2008**, *130*, 756–762.
(17) Helfrich, M. R.; Mangeney-Slavin, L. K.; Djoko, K. Y.; Keating, C. D. *J. Am. Chem. Soc.* **2002**, *124*, 13374–13375.
(18) Albertsson, P. A. *Partition of Cell Particles and Macromolecules*, 2nd ed.; Wiley-Interscience: New York, 1971.
(19) Walter, H.; Johansson, G. *Methods Enzymol.* **1994**, *228*.
(20) Zaslavsky, B. Y. *Aqueous Two-Phase Partitioning: Physical Chemistry and Bioanalytical Applications*; Marcel Dekker: New York, 1995.

10.1021/ja710746d CCC: $40.75

~15 wt % total polymer (7−8% PEG 8 kDa, and 7−10% dextran 10 kDa). For comparison, the cytoplasm has between 17 and 35 wt % macromolecules.[21]

Bulk PEG/dextran ATPS have an upper, PEG-rich aqueous phase and a lower, dextran-rich aqueous phase. Here, and in previous work,[15–17] we take advantage of slight changes in the phase diagram (i.e., in the polymer compositions required for phase separation) that occur as a function of temperature to encapsulate coexisting PEG-rich and dextran-rich microvolumes within giant lipid vesicles (GVs). For the lipid and polymer compositions used here, this results in formation of ATPS-containing GVs (ATPS/GVs) in which an interior dextran-rich aqueous phase is surrounded by an outer PEG-rich aqueous phase.[16] Solutes such as proteins added to ATPS can preferentially accumulate into one of the phases; separations are possible for solutes with different partitioning behavior.[15,16,18–20,22] We have used partitioning between the coexisting PEG-rich and dextran-rich microvolumes to control local protein concentrations within these model cells.[15,16]

Exposure to hypertonic sucrose solutions results in osmotic shrinkage of the ATPS/GVs, which has several consequences. The reduction of volume generates excess membrane area, facilitating deformation to form nonspherical geometries. Concentration of the PEG and dextran polymers inside the vesicle improves solute partitioning between the aqueous phases and increases the interfacial tension at the aqueous-aqueous interface between the PEG-rich and dextran-rich microvolumes.[15,16] This increased interfacial tension, coupled with the excess membrane surface area, can result in expulsion of the interior dextran-rich aqueous phase from within the PEG-rich phase to form one or more "buds" on a PEG-rich GV "body".[16] Since the contents of the aqueous phases are chemically distinct, budding generates compositional asymmetry in the synthetic cytoplasm. When proteins such as soybean agglutinin were partitioned into the dextran-rich phase, this asymmetry led to differences in protein concentration in the buds as compared with the body of the vesicles, a primitive model of polarity.[16]

Herein, we report localization of lipid membrane microdomains in response to the local composition of our ATPS cytoplasm mimic within the vesicles. We accomplished this by building on the chemical asymmetry of the aqueous interior of budded ATPS/GVs to control the location of lipid domains in the vesicle membrane, generating asymmetry in membrane chemistry. Lipid domains presenting PEGylated headgroups preferentially coated the PEG-rich aqueous microvolumes of the budded ATPS/GVs. The resulting model cells exhibit chemical polarity in both their exterior membrane and interior aqueous compositions. Such interplay between internal and external microcompartmentation seems not only possible, but likely, in biological cells.

Results and Discussion

We prepared ATPS-containing GVs by gentle hydration[23] in warm polymer solutions as described previously,[16] except that here we used lipid compositions capable of forming micrometer-scale fluid domains (detailed Methods in Supporting Information). Briefly, polymer concentrations for the ATPS to be encapsulated within the vesicles were determined by examination of the phase diagram for PEG 8 kDa/dextran 10 kDa in water at 4 and 37 °C. ATPS compositions were selected such that the solution would exist as a single phase at 37 °C and as two phases at 4 °C. GVs were prepared by gentle hydration of ternary lipid mixtures in these polymer compositions at 37 °C. The lipid composition used in this work (1:1 DOPC/DPPC[24] + 30% cholesterol) was selected based on phase diagrams for ternary lipid mixtures reported by the Keller group.[10,25] This lipid mixture displays phase coexistence for the liquid ordered (L_o) and liquid disordered (L_d) phases, which form micrometer-scale domains in GVs for a range of lipid compositions.[10,25,26] Our earlier work on ATPS/GV budding indicated that the membrane flexibility contributed by PEGylated headgroups facilitated formation of budded geometries.[16] We therefore modified the 1:1 DOPC/DPPC + 30% cholesterol recipe by including lipids with PEGylated headgroups (2.2% PEG-DPPE). We also added fluorescent lipids to track the location of the domains: 0.1% rhodamine-DOPE, which is known to partition into the DOPC-rich L_d domain,[27] and 0.05% carboxyfluorescein (CF) labeled PEG 2000-modified DSPE (0.05% CF-PEG-DSPE), to report on the distribution of PEGylated lipids.

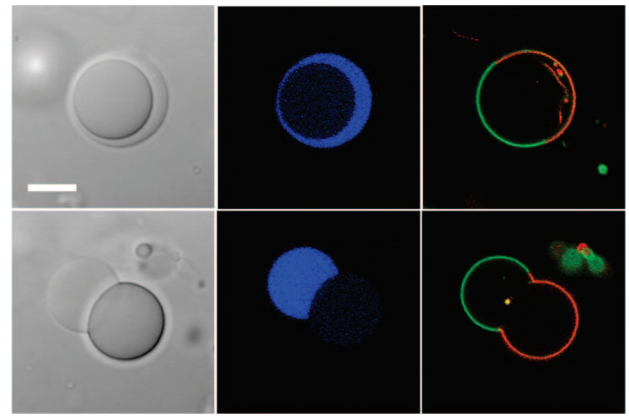

Figure 1. ATPS-containing GV before (top) and after (bottom) budding was induced by osmotic stress. Fluorescence images have been false colored: blue indicates Alexa647, red indicates rhodamine, green indicates CF. Images: transmitted light DIC (left), Alexa 647-labeled PEG 5 kDa fluorescence (center), overlay of rhodamine-DOPE and CF-PEG-DSPE fluorescence images (right). $T = 4$ °C. Scale bar is 10 μm.

After ATPS/GV formation at 37 °C, samples were cooled to 4 °C. At this temperature, the aqueous polymer solution phase separated both in the bulk and in the GV interiors. The resulting ATPS-containing GVs (ATPS/GVs) were collected from the bulk ATPS interface and placed into a sucrose solution on the microscope slide. Confocal fluorescence images of an ATPS/GV are shown in Figure 1. The top panel shows an ATPS-containing GV in isotonic external solution. Two coexisting

(21) Fulton, A. B. *Cell* **1982**, *30*, 345–347.
(22) Long, M. S.; Keating, C. D. *Anal. Chem.* **2006**, *78*, 379–386.
(23) (a) Yamashita, Y.; Oka, M.; Tanaka, T.; Yamazaki, M. *Biochim. Biophys. Acta* **2002**, *1561*, 129–134. (b) Szleifer, I.; Gerasimov, O. V.; Thompson, D. H. *Proc. Natl. Acad. Sci. U.S.A.* **1998**, *95*, 1032–1037. (c) Akashi, K.-I.; Miyata, H.; Itoh, H.; Kinosita, K., Jr. *Biophys. J.* **1996**, *71*, 3242–3250.
(24) Abbreviations: DOPC, 1,2-dioleoyl-*sn*-glycero-3-phosphocholine; DPPC, 1,2-dipalmitoyl-*sn*-glycero-3-phosphocholine; rhodamine-DOPE, 1,2-di-oleoyl-*sn*-glycero-3-phosphoethanolamine-*N*-lissamine rhodamine B sulfonyl; PEG-DPPE, 1,2-dipalmitoyl-*sn*-glycero-3-phospho-ethanolamine-*N*-[methoxy(polyethylene glycol)$_{2000}$]; CF-PEG-DSPE, 1,2-distearoyl-*sn*-glycero-3-phosphoethanolamine-*N*-[poly(ethylene glycol)$_{2000}$-*N*-carboxyfluorescein].
(25) Veatch, S. L.; Polozov, I. V.; Gawrisch, K.; Keller, S. L. *Biophys. J.* **2004**, *86*, 2910–2922.
(26) Veatch, S. L.; Keller, S. L. *Phys. Rev. Lett.* **2002**, *89*, 268101−1268101−4.
(27) Baumgart, T.; Hunt, G.; Farkas, E. R.; Webb, W. W.; Feigenson, G. W. *Biochim. Biophys. Acta* **2007**, *1768*, 2182–2194.

aqueous microvolumes corresponding to the PEG-rich and dextran-rich phases of the ATPS can be seen inside the GV both in the differential interference contrast (DIC) transmitted light image (left) and in the Alexa647-PEG 5 kDa fluorescence image (center). PEG-rich and dextran-rich aqueous phases can be distinguished in DIC images due to slight differences in refractive index and the optical activity of the dextran polymer; the dextran-rich aqueous phase appears "thicker" in the DIC images. Unambiguous assignment of aqueous phase identities was achieved by addition of fluorescently labeled PEG 5 kDa (Figure 1, center). For this vesicle, the outer PEG-rich aqueous phase contacted the membrane and completely surrounded the inner dextran-rich phase. This morphology is typical for ATPS/GV with PEG-modified lipids.[16]

The right-hand panel of Figure 1 shows the location of fluorescently labeled lipids; red indicates rhodamine-DOPE and green indicates CF-PEG-DSPE. The clear separation of red and green regions indicates that our addition of PEG-DPPE and CF-PEG-DSPE did not inhibit the formation of micrometer-scale domains; a slight orange tint to the red regions is due to some green emission in these areas. Partitioning of the rhodamine-labeled DOPE into one of the membrane domains, which we assign as the less ordered, DOPC-rich L_d domain based on the known partitioning of this dye,[27,28] appeared to be essentially complete: no rhodamine-DOPE signal could be detected from the other domain. The CF-labeled, PEGylated lipids partitioned into the DPPC/cholesterol-rich, more ordered domain of the lipid membrane (L_o). Fluorescent labels that partition into L_o are uncommon; even molecules with saturated acyl chains (e.g., Texas Red-DPPE) often partition into L_d due to the presence of the dye moiety on the headgroup.[27] The partitioning of CF-PEG-DSPE into the L_o domain observed here is presumably enabled by the long, flexible PEG chain (2000 Da, 45 monomers) that separates the CF from the lipid headgroup. For this vesicle (Figure 1, top), CF-PEG-DSPE was present in both L_o and L_d, with $\sim 3.5\times$ higher intensity observed in L_o. We note that CF is notoriously sensitive to local environment and can self-quench at high concentrations.[29] However, the amount of dye used here is low, and since the CF is separated from the headgroups by the PEG chain, it may not experience a difference in local environment. Our data are consistent with the expected preference of DSPE tailgroups for the L_o membrane domain and with reduced partitioning due to steric repulsions between PEG 2 kDa headgroup labels. Based on the anticipated equal areas for L_o and L_d domains for this lipid composition,[30] and assuming identical partitioning between L_o and L_d for our 2.25 total mol % (labeled + unlabeled) PEG 2 kDa modified lipids, we can estimate from the apparent CF-PEG-DSPE partitioning that the mole fraction PEG-lipid is $\sim 3.9\%$ in L_o and $\sim 1.1\%$ in L_d. Lipids with polymers such as PEG grafted to their headgroups can exist in two basic regimes based on headgroup density.[31–33] At low densities, the polymers are not close enough to interact with each other, and behave as independent random coils ("mushrooms") extending from the membrane. At higher densities, polymers are close enough to interact with each other and more fully coat the surface, and hence take on a brushlike morphology, extending out further from the membrane. The mushroom-to-brush transition for PEG 2 kDa lipids is at mole fractions of 0.014 (1.4 mol %).[32] Thus, our estimated PEG headgroup densities suggest that PEGylated headgroups in the L_o domain exist as a continuous brush, while those in L_d are in the mushroom regime.

After acquiring the image shown in Figure 1 (top), budding of the ATPS/GV was induced by addition of a sucrose solution of higher osmolarity than the ATPS used to prepare the vesicles. We recently described osmotically induced budding in ATPS/GVs that lack membrane domains (prepared using DOPC/DOPG and DOPC/PEG lipids).[16] Although the interior ATPS is not necessary to osmotically induce GV budding,[34–37] it does impact the final budded geometries. Budding morphologies were observed when ATPS/GVs were dehydrated via osmotic shock, concentrating the ATPS (which increases the interfacial tension at the aqueous/aqueous boundary, a driving force for minimizing the contact of the PEG-rich and dextran-rich phases) and decreasing the GV volume (increasing excess membrane area, and facilitating formation of higher surface area budded morphologies). Importantly, budded ATPS/GV structures have both the PEG-rich and the dextran-rich interior aqueous microvolumes in contact with the lipid membrane, while spherical structures generally do not. In Figure 1 (top), the initial ATPS/GV had the PEG-rich aqueous phase completely surrounding the dextran-rich phase, such that only the PEG-rich volume contacts both L_o and L_d membrane domains prior to the budding event.

In the budded ATPS/GV (Figure 1, bottom), the CF-PEG-DSPE rich L_o membrane domain was localized around the PEG-rich aqueous phase, and the rhodamine-DOPE rich lipid domain (L_d) surrounded the dextran-rich aqueous phase. Inside the vesicle, partitioning of the Alexa647-labeled PEG into the PEG-rich aqueous phase improved from $K = 5 \pm 1$ to 8 ± 2.5 upon budding, where the partitioning coefficient, K, is the concentration ratio of solute in the PEG-rich to dextran-rich aqueous phase. This is due to increased ATPS concentration with osmotic shrinkage; we have previously reported on the use of osmotic shrinkage to improve K for solutes such as proteins in the interior of budded ATPS/GVs.[15,16] For this GV, we observed a 22% volume loss; for the 8% PEG 8 kDa/8% dextran 10 kDa ATPS used here, this would result in concentration to ~ 10 wt % of each polymer, which according to the PEG/dextran/water phase diagram cannot be converted back to a single aqueous phase by moderate heating (i.e., <50 °C).[38]

(28) Veatch, S. L.; Keller, S. L. *Biophys. J.* **2003**, *85*, 3074–3083.
(29) Haugland, R. P. *Handbook of Fluorescent Probes and Research Products*, 9th ed.; Molecular Probes Inc.: Eugene, OR, 2002.
(30) Beattie, M. E.; Veatch, S. L.; Stottrup, B. L.; Keller, S. L. *Biophys. J.* **2005**, *89*, 1760–1768.
(31) de Gennes, P. G. *Macromolecules* **1980**, *13*, 1069–1075.
(32) Marsh, D.; Bartucci, R.; Sportelli, L. *Biochim. Biophys. Acta* **2003**, *1615*, 33–59.
(33) Milner, S. T. *Science* **1991**, *251*, 905–914.
(34) (a) Dobereiner, H.-G.; Kas, J.; Noppl, D.; Sprenger, I.; Sackmann, E. *Biophys. J.* **1993**, *65*, 1396–1403. (b) Kas, J.; Sackmann, E. *Biophys. J.* **1991**, *60*, 825–844.
(35) Kumar, P. B. S.; Gompper, G.; Lipowsky, R. *Phys. Rev. Lett.* **2001**, *86*, 3911–3914.
(36) Bernard, A.-L.; Guedeau-Boudevile, M.-A.; Jullien, L.; di Meglio, J.-M. *Biochim. Biophys. Acta* **2002**, *1567*, 1–5.
(37) Boroske, E.; Elwenspoek, M.; Helfrich, W. *Biophys. J.* **1981**, *34*, 95–109.
(38) An additional change upon osmotically induced shrinkage in Figure 1 is worth noting: the interior lipid material seen in the top panel has condensed and moved to the ATPS interface in the lower panel. This is consistent with increased interfacial tension at the aqueous/aqueous phase boundary due to concentration of the ATPS, increasing the driving force for particle collection.[18,51] Additionally, increased macromolecular crowding within each of the aqueous phases[52,53] may play a role in condensation of the lipid material. Collection of lipid material at the ATPS interface within pre-formed ATPS/GV may provide a route to separating the two aqueous microcompartments, a step toward a primitive model of cell division.

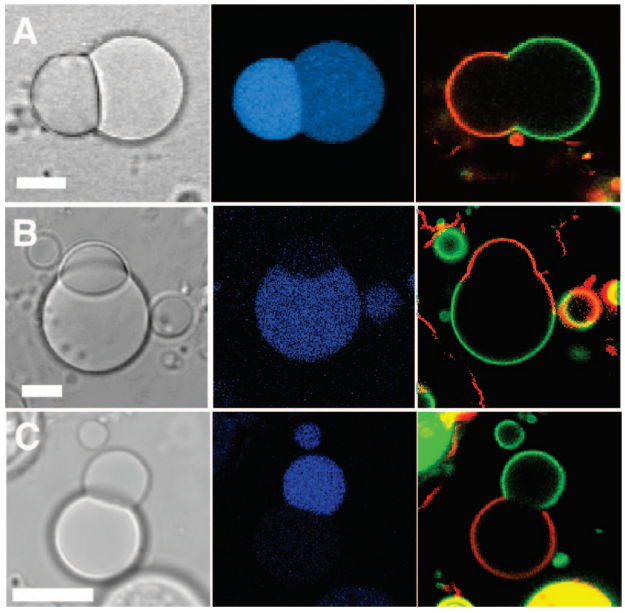

Figure 2. Confocal optical microscopy images of interior aqueous polymer and external lipid and composition asymmetry in budded, ATPS-containing giant vesicles. Polymer partitioning in the interior ATPS was visualized by Alexa647-labeled dextran 10 kDa (A) or Alexa-labeled PEG 5 kDa (B,C). Images have been false colored: blue indicates Alexa647, red indicates rhodamine, green indicates CF. Panels: transmitted light DIC (left), Alexa 647-labeled polymer fluorescence, (center), overlay of rhodamine-DOPE and CF-PEG-DSPE images (right). $T = 4$ °C in (A) and (B), and $T = 6$ °C in (C). All scale bars are 10 μm.

Additional examples of budded ATPS/GVs with L_o/L_d coexistence are shown in Figure 2. The GV in Figure 2A was labeled with Alexa647-dextran 10 kDa (0.008%), while those in Figure 2B,C were labeled with Alexa647-PEG 5 kDa (0.02%). The partitioning of dextran 10 kDa is not as strong as that of PEG 5 kDa in these ATPS; this can be seen in the partitioning of the Alexa647 PEG 5 kDa in Figure 1 and 2B,C, as compared with that for dextran 10 kDa partitioning for the vesicle in Figure 2A. DIC and fluorescence images indicate that the dextran-rich phase has a smaller volume than the PEG-rich aqueous phase for the GV in Figure 2A,B, and the dextran-rich aqueous microvolume was larger in Figure 2C.

The structures described here differ in two important ways from previously reported liposome structures comprising lipid domains with polymer-free aqueous interiors.[10,39–41] First, they contain coexisting interior aqueous microcompartments, each contacting different regions of the lipid membrane, such that not only the membrane, but also the model cytoplasm is chemically asymmetric. Second, the overall shape of the ATPS-filled GVs is governed primarily by the internal aqueous phases rather than by the line tension between, or differences in mechanical properties of, the lipid domains. This can be observed in Figure 2B, as well as the lower panel of Figure 1, where the (red) L_d lipid phase is larger than required to encapsulate the dextran-rich bud, and also partially coats the PEG-rich GV body. The degree to which this occurs depends in part on the relative sizes of aqueous to lipid domains, which can be altered via the lipid and polymer compositions during preparation. We anticipate that line tension between, and mechanical properties of, L_o and L_d, as well as interfacial tension at the ATPS boundary between the dextran-rich and PEG-rich aqueous phases also impact the observed morphologies. For the recipes used here, the ATPS composition leads to ~2:1 volume ratio of PEG-rich to dextran-rich aqueous phase volumes in bulk, and similar mean volume ratio for GV-encapsulated ATPS, although the relative sizes of the aqueous phases varies for individual vesicles within a batch.[15] Because the lipid composition used leads to roughly equal L_d and L_o domain areas,[30] we generally see L_d phase domains that are larger than needed to coat the dextran-rich internal microvolume.

Possible explanations for the observed positioning of L_o and L_d lipid membrane domains around the PEG-rich and dextran-rich interior aqueous microvolumes include (1) differences in mechanical properties of the two L_d and L_o membrane domains, such that L_d, which has lower bending rigidity,[42,43] prefers to surround the higher curvature (i.e., smaller volume) dextran-rich bud; (2) interactions between lipid headgroups and the interior aqueous polymer solutions, e.g., PEGylated headgroups with PEG and dextran polymers; or (3) greater deformability of the L_d membrane domain, such that when budding occurs by expulsion of the interior dextran-rich microvolume from the body of the vesicle, the bud protrudes from this more flexible portion of the membrane. We will evaluate each of these possibilities below.

Two of the three possible explanations for the observed pinning of L_o and L_d membrane domains around PEG-rich and dextran-rich interior aqueous phases involved differences in mechanical properties between L_o and L_d lipid phase domains. The L_d domain is known to be more readily deformed than the L_o domain for DOPC/DPPC/cholesterol membranes;[42] however, the effect of adding PEGylated headgroups to these ternary mixtures has not been evaluated. Our hypotheses (1) and (3) above assume no major effect on the relative rigidities of L_o vs L_d from the 2.25 mol % PEGylated lipids. We note that this ignores any impact the presence and nonuniform distribution of PEGylated headgroups may have on L_d vs L_o mechanical properties. PEGylated headgroups are known to effect membrane mechanical properties, inducing membrane area expansion and altering bending elastic moduli.[44–46] We have found that osmotically induced budding in ATPS/GVs with single-domain DOPC/DOPG membranes is favored by addition of PEGylated lipid, with increasing % budded vesicles as the mushroom-to-brush transition was approached.[16] However, addition of 40% cholesterol, which increases membrane stiffness,[9,47] to the DOPC/DOPG membranes inhibited budding.[16] Thus, the increased flexibility provided by PEGylated lipids can be expected to affect L_d domains to a greater degree than the cholesterol-rich L_o domains, and therefore we anticipate that for our PEG-decorated membranes, L_o remains more rigid than L_d.

Hypothesis (1). Can the observed structures be explained as the L_o domains coating the region of lower curvature, which due to its larger volume is generally the PEG-rich vesicle body? Coexisting L_d and L_o lipid membrane phase domains are known to result in budded GV structures where buds are composed of

(39) Baumgart, T.; Hess, S. T.; Webb, W. W. *Nature* **2003**, *425*, 821–824.
(40) Julicher, F.; Lipowsky, R. *Phys. Rev. E* **1996**, *53*, 2670–2683.
(41) Bacia, K.; Schwille, P.; Kurzchalia, T. *Proc. Natl. Acad. Sci. U.S.A.* **2005**, *102*, 3272–3277.
(42) Baumgart, T.; Das, S.; Webb, W. W.; Jenkins, J. T. *Biophys. J.* **2005**, *89*, 1067–1080.
(43) Parthasarathy, R.; Groves, J. T. *Soft Matter* **2007**, *3*, 24–33.
(44) Marsh, D. *Biophys. J.* **2001**, *81*, 2154–2162.
(45) Tribet, C.; Vial, F. *Soft Matter* **2008**, *4*, 68–81.
(46) (a) Lipowsky, R. *Colloids Surf. A* **1997**, *128*, 255–264. (b) Bivas, I.; Winteralter, M.; Meleard, P.; Bothorel, P. *Europhys. Lett.* **1998**, *41*, 261–266.
(47) Song, J.; Waugh, R. E. *Biophys. J.* **1993**, *64*, 1967–1970.

different lipid domains than the vesicle body; these structures arise due to differences in mechanical properties between the two domains and from the line tension between them.[39–41] In the ATPS/GV described here, the buds clearly form via a different mechanism, since they do not necessarily correspond to the different lipid domains, but rather to the interior polymer-rich microdomains of the encapsulated ATPS. This can be seen, for example, in Figure 2B, where the L_d domain is larger than required to coat the dextran-rich bud, and thus partially coats the PEG-rich body of the ATPS/GV. The more flexible L_d membrane domain[42] might be expected to localize onto the dextran-rich buds due to their greater curvature (smaller volume). However, our data exclude this explanation; when the relative sizes of PEG-rich and dextran-rich aqueous microvolumes are reversed, L_d still coats the dextran-rich interior volumes, while the PEGylated L_o membrane domain still coats the interior PEG-rich domain (Figure 2C).

The data in Figures 1 and 2 are consistent with interpretation (2) above, i.e., that chemical interactions between the PEG-rich interior aqueous phase and the PEGylated lipid headgroups concentrated in the L_o membrane domain drive the observed positioning of membrane domains. In addition to the positioning of the PEGylated L_o membrane domain around the PEG-rich aqueous bud, the apparent localization of the CF-PEG-DSPE lipid into L_o improved nearly 2-fold upon budding (from a fluorescence intensity ratio for the CF-PEG-DSPE in L_o/L_d of $K_{PEG\text{-}DSPE} = 2.2 \pm 0.4$ before to 4 ± 1 after budding). This increase in apparent CF-PEG-DSPE lipid partitioning into the L_o membrane domain can be interpreted as a reaction to the change from both domains (L_o and L_d) contacting only the PEG-rich interior aqueous microvolume prior to budding, to these domains contacting primarily the PEG-rich and dextran-rich microvolumes, respectively, after budding. In bulk PEG/dextran ATPS, incorporation of DSPE-PEG in small unilamellar vesicles (~120 nm) results in strong partitioning of the PEGylated SUVs into the PEG-rich aqueous phase.[48] In our ATPS/GVs, we cannot entirely rule out the possibility that the decrease in membrane area (~9%) upon budding itself contributes to the change in $K_{PEG\text{-}DSPE}$. Although the separation of the CF moiety from the lipid headgroup by the PEG 2 kDa presumably shields the dye itself from large changes in local environment, steric interactions between adjacent PEGylated headgroups may be impacted by this change in membrane area, which could alter the distribution of CF-PEG-DSPE.

These data cannot rule out possibility (3) above, where buds exit the body of the vesicle at the point where mechanical deformation of the membrane is most facile (i.e., L_d domains). We evaluated this possibility by moving the PEGylated headgroups from the L_o to the L_d domain. By incorporating PEG2000-DOPE and omitting the PEG2000-DPPE and CF-PEG2000-DSPE used in the experiments described above (Figures 1 and 2), it was possible to localize the L_d phase domain around the PEG-rich aqueous microvolume. Figure 3 shows DIC and conventional fluorescence optical microscope images for a budded ATPS/GV in which PEGylated headgroups were included on lipids targeting the L_d membrane phase domain. Here, green fluorescence indicates FITC-labeled dextran polymer in the aqueous phase, and red fluorescence indicates DOPE-rhodamine, labeling the L_d domain of the lipid membrane. When the L_d domain lipid presents PEG moieties, it is localized to the (unlabeled) PEG-rich microvolume. Thus, despite the more facile deformability of the PEGylated L_d domain, the dextran-rich bud in this vesicle is surrounded by the L_o membrane domain. We note that both the higher PEG headgroup density and the mechanical properties of L_d without PEGylated lipid suggest that the PEGylated L_d domain is more readily deformed; the dextran bud nonetheless occurs at the L_o domain in this experiment. These data argue against membrane mechanical properties, and for polymer−polymer interactions, in determining the locations of L_d and L_o membrane domains with respect to interior PEG-rich and dextran-rich aqueous microvolumes.

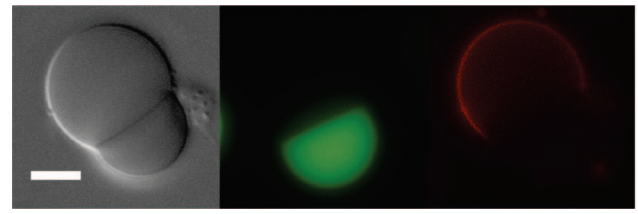

Figure 3. Optical microscope images for ATPS/GV where L_d lipid domain harbors the PEG2000 functionalization. GVs were prepared with 1:1 DOPC: DPPC + 30% cholesterol, and 2.2% DOPE-PEG2000, and imaged at 7 °C. The L_d phase of the vesicles was stained with 0.1% DOPE-rhodamine and is false colored red in the fluorescent images; the L_o phase was not labeled and appears dark. We also added 0.05% FITC-labeled dextran 500 kDa (green) to facilitate identification of the dextran-rich aqueous phase. The DOPE-PEG2000 is targeted to the L_d phase (red); the L_d phase coated the nonlabeled PEG enriched bud and the L_o phase the dextran bud. Scale bar is 10 μm.

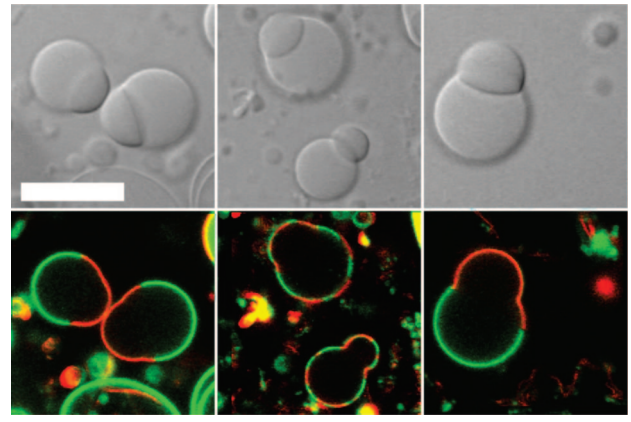

Figure 4. Effect of temperature on membrane domain localization in ATPS-containing GV. Different regions of the sample are shown initially at 4 °C (left), after heating to 35 °C (center), and subsequent cooling to 4 °C (right). Top panel is transmitted light, DIC; bottom panel is overlay of rhodamine-DOPE and CF-PEG-DSPE fluorescence. Fluorescence images have been false colored: red indicates rhodamine, and green indicates CF. Scale bar is 50 μm.

Further support for the role of internal aqueous polymer composition on membrane domain positioning comes from the behavior of these ATPS/GVs when exposed to changes in temperature. Figures 4 and 5 show the effect of temperature. The vesicles in Figure 4 show the typical morphology for the ATPS/GV recipes used here, with a smaller volume dextran-rich bud and a larger PEG-rich vesicle "body"; the dextran-rich phase appears denser in the DIC transmitted light images. Here, different representative vesicles from the same sample are shown at each temperature. The vesicle in Figure 5 was labeled with Alexa647 PEG 5 kDa so that polymer partitioning between the aqueous phases could be monitored, and was followed as the temperature was changed (this is the same

(48) (a) Senior, J.; Selgado, C.; Fisher, D.; Tilcock, C.; Gregoriadis, G. *Biochim. Biophys. Acta* **1991**, *1062*, 77–82. (b) Moribe, K.; Maruyama, K.; Iwatsuru, M. *Chem. Pharm. Bull.* **1997**, *45*, 1683–1687.

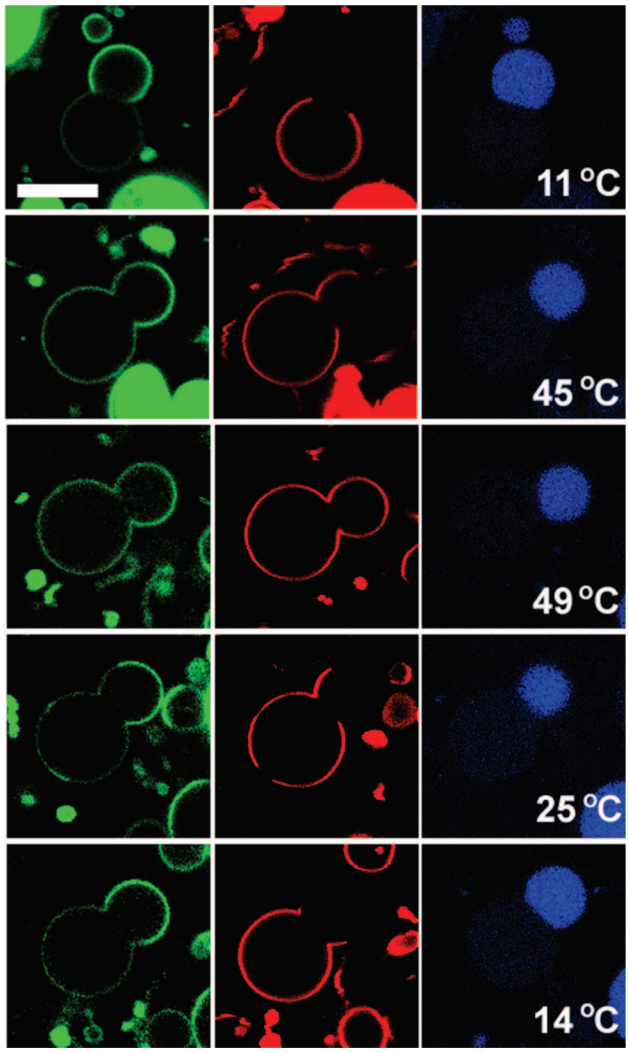

Figure 5. Effect of temperature on membrane domain localization in a single ATPS-containing GV. Fluorescence images have been false colored: green (left panels) indicates CF-PEG-DSPE, red (center panels) indicates rhodamine-DOPE, and blue (right panels) indicates Alexa647 PEG 5 kDa. Scale bar is 10 μm.

vesicle as shown in Figure 2C). Initial images at low temperature, 4 and 11 °C for Figures 4 and 5, respectively, show two coexisting lipid domains, L_o (green) surrounding the PEG-rich aqueous compartments and L_d (red) surrounding primarily the dextran-rich aqueous buds. Heating led first to the fragmentation of the L_o and L_d domains into smaller patches that were no longer pinned to the interior aqueous microvolumes (Figures 4B and 5B). At higher temperatures (49 °C) and longer incubation times (75 min), complete lipid miscibility was observed (Figure 5C).

For the DOPC:DPPC:cholesterol ratio used here, the miscibility temperature (T_{mix}) is 32 ± 1 °C; however, our ATPS/GVs retained some phase separation after ~10 min at 35 °C. Our membrane composition also includes 2.25% PEGylated lipid, which can be expected to impact T_{mix} and/or slow the phase transition by reducing lipid diffusion rates in the membrane. Literature reports on PEGylated lipids added to single component DPPC membranes indicate that while the PEG moieties can lead to slight reductions in the chain melting temperature,[49] when the PEGylated lipid has a longer acyl chain length than the major lipid component (e.g., 18-carbon DSPE vs 16-carbon DPPC), the melting temperature is instead slightly increased.[50] To our knowledge, the effect of PEGylated lipids on ternary DOPC:DPPC:cholesterol mixtures such as were used here has not been investigated. However, minor component lipid impurities can alter T_{misc}. For example, Keller and co-workers have found ~3 °C increase in T_{misc} for a ternary DOPC:brain sphingomyelin:cholesterol system upon addition of 1% ganglioside GM1, which partitions into the L_o domain.[10] Additionally, when impurities accumulate at phase boundaries, they can reduce line tensions and enable domain persistence at elevated temperatures.[10]

Although as noted above, the internal ATPS does not revert to a single phase upon heating because the polymer solution was concentrated during budding and no longer corresponds to the composition during the GV formation process, some reduction in polymer partitioning might be anticipated at elevated temperature. We therefore monitored the fluorescence intensity ratio of Alexa647-PEG 5 kDa in the PEG-rich and dextran-rich aqueous phases. For the ATPS/GV shown in Figure 5, any change in K for the Alexa647 PEG with temperature was not statistically significant, given the error of our measurement ($K = 11 \pm 4$ at 11 °C and 9 ± 2 at 49 °C).

In order to quantify the change in localization of the PEGylated L_o domain to the PEG-rich interior aqueous microvolume that occurred as a function of temperature, we calculated an intensity ratio for CF-PEG-DSPE in the membrane surrounding the PEG-rich vs dextran-rich aqueous phases (R_{PEG}). R_{PEG} was determined by measuring the mean fluorescence intensity for CF-PEG-DSPE in the membrane surrounding the PEG-rich vesicle bodies and dividing by the mean intensity around the dextran-rich buds. This value is not a partitioning constant, but rather an estimate of PEGylated lipid location with respect to the interior aqueous compartments. Twenty ATPS/GVs were analyzed at 4 and 35 °C, from the sample shown in Figure 4. We found $R_{PEG} = 4 \pm 1$ initially at 4 °C and $R_{PEG} = 1.0 \pm 0.1$ after heating to 35 °C. Because even at 35 °C, L_o and L_d membrane domains remained, and most of the CF-PEG-DSPE was concentrated in the L_o domains, R_{PEG} also indicates the position of the L_o domains with respect to interior PEG-rich vs dextran-rich volumes. At 4 °C, part of the L_d membrane domains, which are localized around the dextran-rich buds, extend onto the PEG-rich vesicle bodies as a consequence of the size mismatch between internal volumes and the membrane domains. At 35 °C, L_o and L_d patches were distributed evenly around the budded GVs. This suggests that the interaction between PEGylated lipids concentrated in the L_o regions and the free PEG polymer molecules concentrated in the PEG-rich phase of the vesicle interior is of relatively low affinity, and is overcome by heating to 35 °C. Subsequent cooling back to 4 °C, restored the L_o and L_d membrane domains to their positions around the PEG-rich and dextran-rich internal aqueous microvolumes, respectively, with $R_{PEG} = 3.5 \pm 0.4$. The reversible pinning of lipid domains by the internal aqueous domains

(49) Pantusa, M.; Bartucci, R.; Marsh, D.; Sportelli, L. *Biochim. Biophys. Acta* **2003**, *1614*, 165–170.

(50) (a) Baekmark, T. R.; Pederson, S.; Jorgensen, K.; Mouritsen, O. G. *Biophys. J.* **1997**, *73*, 1479–1491. (b) Hashizaki, K.; Itoh, C.; Sakai, H.; Yokoyama, S.; Taguchi, H.; Saito, Y.; Ogawa, N.; Abe, M. *Colloids Surf. B: Biointerfaces* **2000**, *17*, 275–282.

(51) Helfrich, M. R.; El-Kouedi, M.; Etherton, M. R.; Keating, C. D. *Langmuir* **2005**, *21*, 8478–8486.

(52) Zimmerman, S. B.; Minton, A. P. *Annu. Rev. Biophys. Biomol. Struct.* **1993**, *22*, 27–65.

(53) Ellis, R. J. *Trends Biochem. Sci.* **2001**, *265*, 597–604.

demonstrates that lipid domain position is not random, and does not result from the differences in mechanical properties of the L_o and L_d membrane domains but rather is controlled by internal aqueous phase position.

Conclusions

We have demonstrated the interrelationship of interior aqueous and exterior lipid organization in this very simple cytomimetic model. Here, the "pinning" of lipid domains to internal aqueous compartments was caused by nonspecific interactions between PEGylated lipid headgroups and a PEG-rich internal aqueous phase. More complex and/or specific biorecognition schemes could also be used to control lipid phase location with respect to interior aqueous components. Although living cells may not contain simple micrometer-scale aqueous or lipid domains like those used here, the cytoplasm and plasma membranes are characterized by heterogeneity, which via specific or nonspecific interactions with lipid headgroups, glycolipids, or membrane proteins could be expected to organize similarly to what we observed here with this very simple model system.

Acknowledgment. We thank the National Science Foundation (CHE-0239629) and Penn State University for financial support. A-S.C. thanks the Knut and Alice Wallenberg Foundation for a postdoctoral fellowship. C.D.K. acknowledges support from a Beckman Young Investigator award, a Sloan Fellowship, and a Dreyfus Teacher-Scholar Award.

Supporting Information Available: Experimental methods. This material is available free of charge via the Internet at http://pubs.acs.org.

JA710746D